Electronic Supplementary Materials

Sample preparation:

The $(Mg_{0.37}Mn_{0.32}Fe_{0.31})CO_3$, $(Fe_{0.51}Mg_{0.49})CO_3$, $(Mn_{0.53}Fe_{0.47})CO_3$, $(Mg_{0.50}Mn_{0.50})CO_3$, $FeCO_3$, $MgCO_3$ and $MnCO_3$ single crystals were prepared by high *P-T* annealing as reported by Liang *et al*. (2018a) . The high *P-T* reactions were performed on a DS 6×600t cubic-anvil-type apparatus using *h*-BN pressure medium and a graphite heater. MgO (99.99%, Alfa Aesar), Fe_2O_3 (99.99%, Alfa Aesar), $MnCO_3$ (99.99%, Alfa Aesar), and anhydrous $H_2C_2O_4$ (98%, Alfa Aesar) were used as starting materials to participate in the annealing reaction:

$$0.5MgO+0.25Fe_2O_3+1.5H_2C_2O_4 \rightarrow (Mg_{0.5}Fe_{0.5})CO_3+ (CO+CO_2\ \text{atmosphere})$$

$$0.5MgO+0.5MnCO_3+1.5H_2C_2O_4 \rightarrow (Mg_{0.5}Mn_{0.5})CO_3+ (CO+CO_2\ \text{atmosphere})$$

$$0.25Fe_2O_3+0.5MnCO_3+1.5H_2C_2O_4 \rightarrow (Fe_{0.5}Mn_{0.5})CO_3+ (CO+CO_2\ \text{atmosphere})$$

$$1/3MgO+1/6Fe_2O_3+1/3MnCO_3+1.5H_2C_2O_4 \rightarrow (Mg_{0.33}Fe_{0.33}Mn_{0.0.33})CO_3+ (CO+CO_2\ \text{atmosphere})$$

The annealing reaction with a fully sealed platinum capsule was carried out in the aquatic medium under 3 GPa and 700 °C for 48 h. After the high *P-T* experiment, the quenched sample was removed from the platinum capsule, and the single crystals were optically examined under a plane polarized microscope.

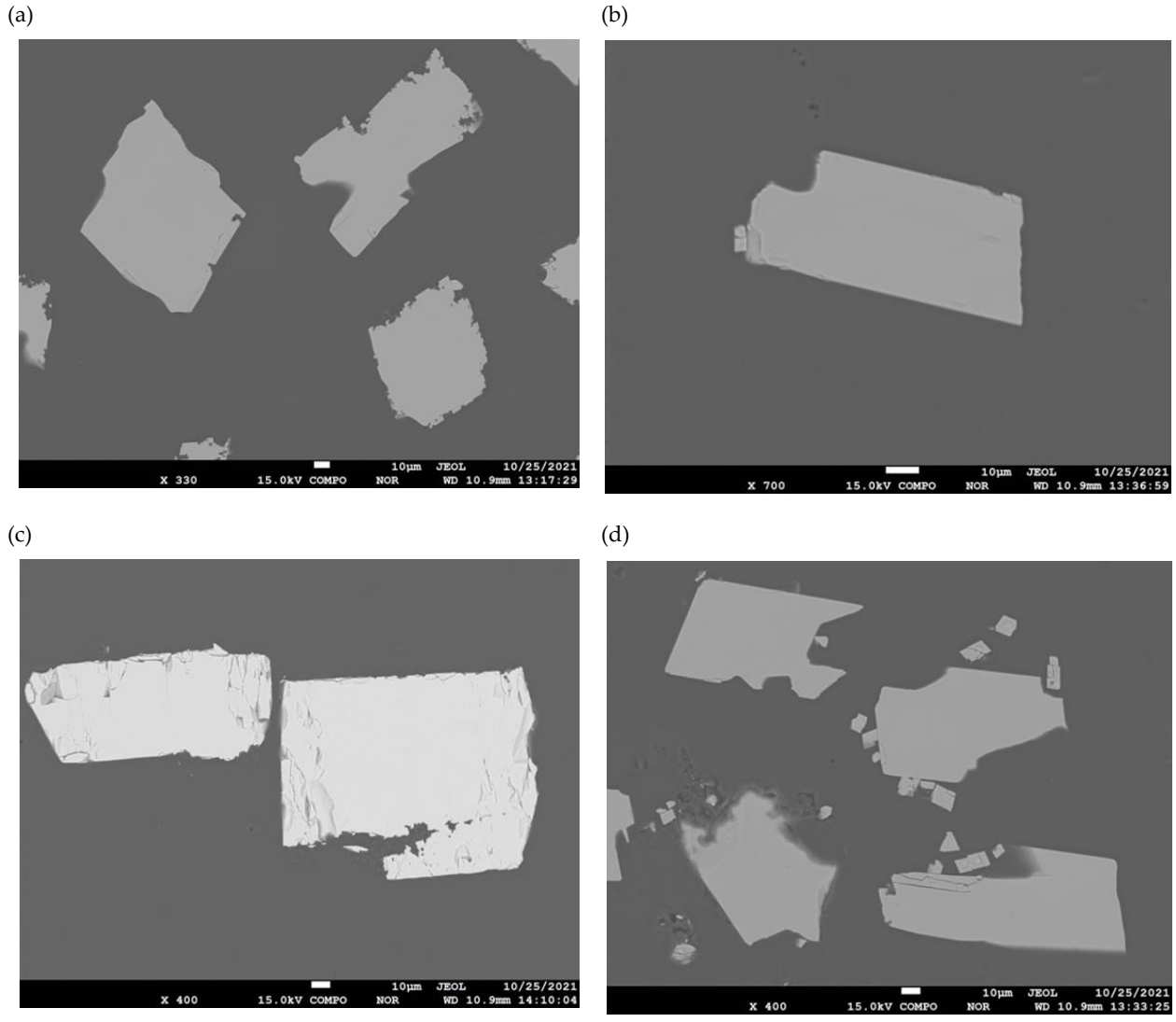

Supplementary Figure S1. The backscattered electronic (BSE) image of single crystal thin sections of (a) $(Mg_{0.37}Mn_{0.32}Fe_{0.31})CO_3$, (b) $(Fe_{0.51}Mg_{0.49})CO_3$, (c) $(Mn_{0.53}Fe_{0.47})CO_3$, and (d) $(Mg_{0.50}Mn_{0.50})CO_3$ in which the red circles are the detection position of electron probing.

The observed vibrational bands of magnesite $MgCO_3$, siderite $FeCO_3$ and rhodochrosite $MnCO_3$ at 300 K were compared with their documented values in Table 1. The positions of the observed Raman bands of magnesite $MgCO_3$ at ambient temperature are similar to those reported by Farsang *et al*., (2018) and Gillet *et al*., (1993), however, the positions of the observed Raman bands of siderite $FeCO_3$ and rhodochrosite $MnCO_3$ are slightly smaller (1-3 cm^{-1} shift) than those reported by Wang *et al*., (2022) and Farsang *et al*., (2018). The minor shift in positions may be attributed to deviations from the stoichiometry, the effect of natural impurities or the presence of point defects. Among all samples, magnesite $MgCO_3$ with the smallest ion radii has the highest Raman wavenumbers.

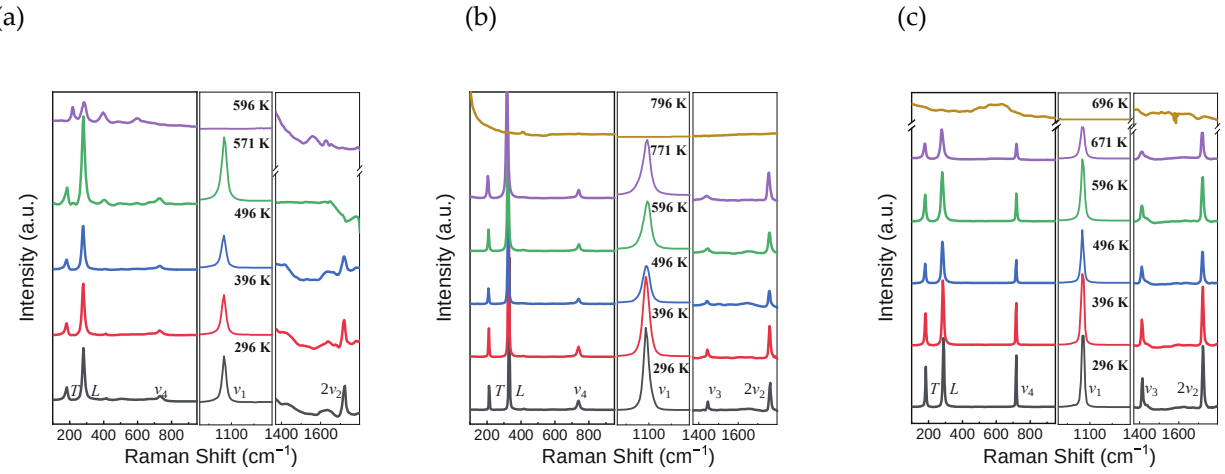

Supplementary Figure S2. Representative Raman spectra of (a) $FeCO_3$, (b) $MgCO_3$ and (c) $MnCO_3$ at high temperature. The asterisks (*) symbolize the unassigned Raman peaks.

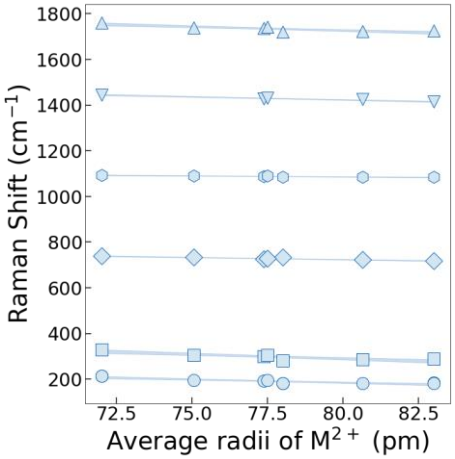

Supplementary Figure S3. Raman shifts of $(Mg_{0.37}Mn_{0.32}Fe_{0.31})CO_3$, $(Fe_{0.51}Mg_{0.49})CO_3$, $(Mn_{0.53}Fe_{0.47})CO_3$, $(Mg_{0.50}Mn_{0.50})CO_3$, $FeCO_3$, $MgCO_3$ and $MnCO_3$ of each mode with the change of average ion radii.

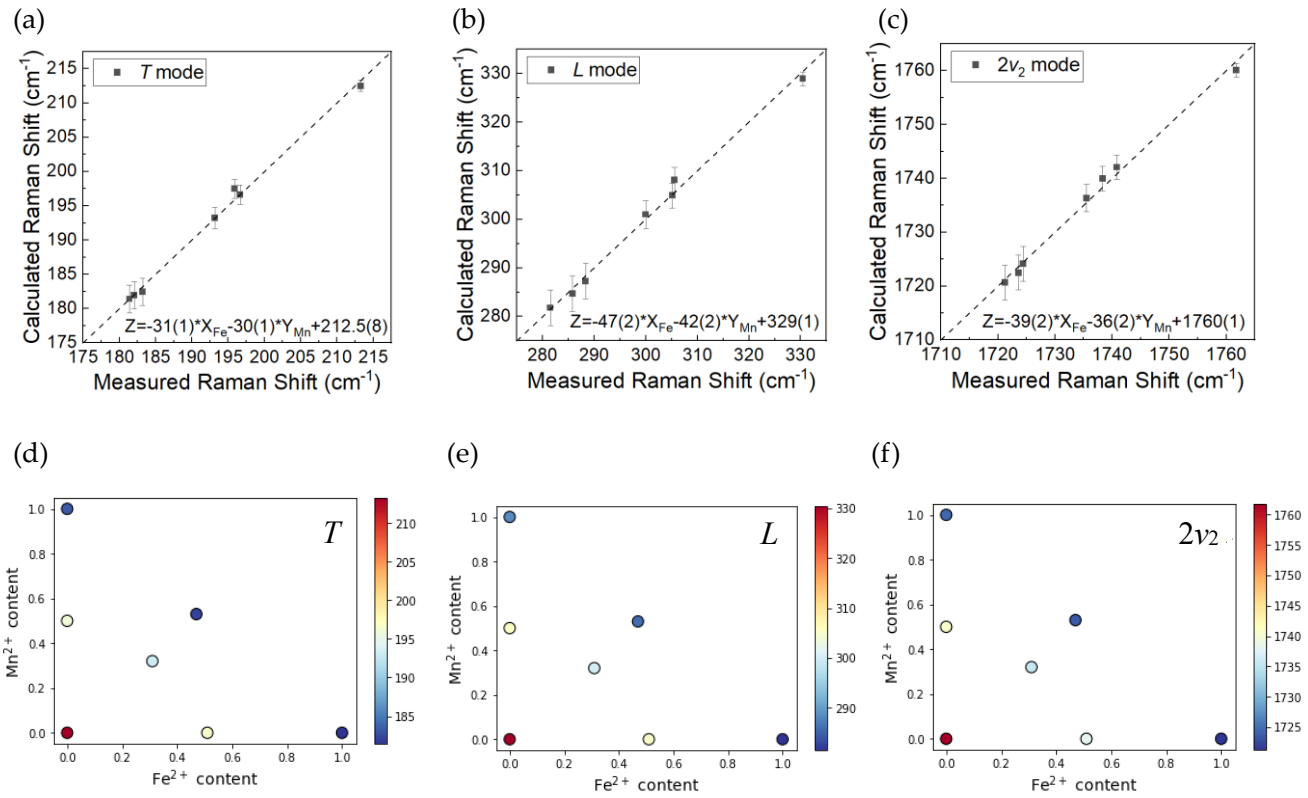

Supplementary Figure S4. The relationship between content of iron and manganese and the Raman shift of mode (a) *T*, (b) *L* and (c) $2v_2$ and the thermal diagram of iron and manganese on the Raman shift of mode (d) *T*, (e) *L* and (f) $2v_2$ at 300K.

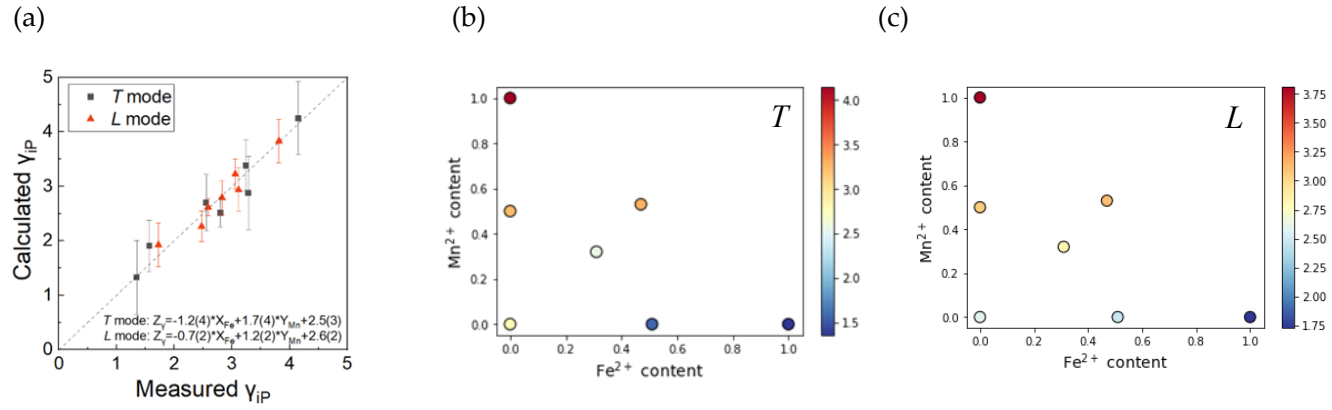

Supplementary Figure S5. (a) The relationship between content of iron and manganese and the mode Grüneisen parameters of mode *T* and *L*. The effect of iron and manganese on the mode Grüneisen parameters of mode (b) *T* and (c) *L*.

Supplementary Table S1. Results of electron probe analysis of single crystal thin sections of Mg-Fe-Mn carbonates.

	Oxides Mass (%)	MgO	MnO	FeO	Composition
Sample 1	Position 1	14.551	22.158	21.581	$Mg_{0.37}Mn_{0.32}Fe_{0.31}CO_3$
	Position 2	15.378	22.654	21.251	$Mg_{0.38}Mn_{0.32}Fe_{0.30}CO_3$
	Position 3	15.003	23.098	20.980	$Mg_{0.38}Mn_{0.32}Fe_{0.30}CO_3$
	Position 4	14.330	22.970	22.476	$Mg_{0.38}Mn_{0.32}Fe_{0.30}CO_3$
	Position 5	14.478	22.647	22.749	$Mg_{0.36}Mn_{0.33}Fe_{0.31}CO_3$
	Position 6	14.442	22.029	22.729	$Mg_{0.36}Mn_{0.32}Fe_{0.32}CO_3$
	Position 7	14.350	22.282	22.224	$Mg_{0.36}Mn_{0.32}Fe_{0.32}CO_3$
	Position 8	14.363	22.585	21.453	$Mg_{0.36}Mn_{0.33}Fe_{0.31}CO_3$
	Position 9	14.033	22.859	22.336	$Mg_{0.35}Mn_{0.33}Fe_{0.32}CO_3$
	Position 10	14.629	22.373	21.969	$Mg_{0.37}Mn_{0.32}Fe_{0.31}CO_3$
	Average	**14.556**	**22.566**	**21.975**	**$Mg_{0.37}Mn_{0.32}Fe_{0.31}CO_3$**
Sample 2	Position 1	19.457	-	37.075	$Fe_{0.52}Mg_{0.48}CO_3$
	Position 2	20.452	-	37.556	$Fe_{0.51}Mg_{0.49}CO_3$
	Position 3	20.008	-	37.207	$Fe_{0.51}Mg_{0.49}CO_3$
	Position 4	20.315	-	37.870	$Fe_{0.51}Mg_{0.49}CO_3$
	Position 5	20.435	-	37.786	$Fe_{0.51}Mg_{0.49}CO_3$
	Position 6	20.558	-	37.826	$Fe_{0.51}Mg_{0.49}CO_3$
	Position 7	20.963	-	37.493	$Fe_{0.50}Mg_{0.50}CO_3$
	Position 8	20.231	-	38.206	$Fe_{0.51}Mg_{0.49}CO_3$
	Position 9	20.806	-	37.791	$Fe_{0.50}Mg_{0.50}CO_3$
	Position 10	20.526	-	37.573	$Fe_{0.51}Mg_{0.49}CO_3$
	Position 11	20.571	-	37.511	$Fe_{0.51}Mg_{0.49}CO_3$
	Position 12	20.849	-	37.969	$Fe_{0.51}Mg_{0.49}CO_3$
	Position 13	20.659	-	37.538	$Fe_{0.50}Mg_{0.50}CO_3$
	Position 14	20.538	-	37.677	$Fe_{0.51}Mg_{0.49}CO_3$
	Position 15	20.501	-	37.164	$Fe_{0.50}Mg_{0.50}CO_3$
	Average	**20.458**	-	**37.616**	**$Fe_{0.51}Mg_{0.49}CO_3$**
Sample 3	Position 1	-	33.923	28.158	$Mn_{0.54}Fe_{0.46}CO_3$
	Position 2	-	33.355	29.822	$Mn_{0.53}Fe_{0.47}CO_3$
	Position 3	-	33.151	28.459	$Mn_{0.54}Fe_{0.46}CO_3$
	Position 4	-	32.689	29.373	$Mn_{0.53}Fe_{0.47}CO_3$
	Position 5	-	33.468	29.359	$Mn_{0.54}Fe_{0.46}CO_3$
	Position 6	-	33.507	29.581	$Mn_{0.53}Fe_{0.47}CO_3$
	Position 7	-	33.753	29.022	$Mn_{0.54}Fe_{0.46}CO_3$
	Position 8	-	33.434	29.686	$Mn_{0.53}Fe_{0.47}CO_3$
	Position 9	-	32.384	29.612	$Mn_{0.53}Fe_{0.47}CO_3$
	Position 10	-	33.007	29.312	$Mn_{0.53}Fe_{0.47}CO_3$
	Average	-	**33.267**	**29.238**	**$Mn_{0.53}Fe_{0.47}CO_3$**

	Position 1	19.727	36.951	-	$Mg_{0.48}Mn_{0.52}CO_3$
	Position 2	19.838	36.535	-	$Mg_{0.49}Mn_{0.51}CO_3$
	Position 3	21.962	34.084	-	$Mg_{0.53}Mn_{0.47}CO_3$
	Position 4	21.225	35.581	-	$Mg_{0.51}Mn_{0.49}CO_3$
	Position 5	20.319	36.348	-	$Mg_{0.50}Mn_{0.50}CO_3$
Sample 4	Position 6	19.756	37.914	-	$Mg_{0.52}Mg_{0.48}CO_3$
	Position 7	20.618	36.749	-	$Mg_{0.50}Mn_{0.50}CO_3$
	Position 8	19.264	37.475	-	$Mg_{0.52}Mg_{0.48}CO_3$
	Position 9	22.415	34.038	-	$Mg_{0.47}Mn_{0.53}CO_3$
	Position 10	22.349	34.368	-	$Mg_{0.47}Mn_{0.53}CO_3$
	Average	**20.899**	**35.805**	-	**$Mg_{0.50}Mn_{0.50}CO_3$**

Supplementary Table S2. Single-crystal XRD parameters of $(Mg_{0.37}Mn_{0.32}Fe_{0.31})CO_3$, $(Fe_{0.51}Mg_{0.49})CO_3$, $(Mn_{0.53}Fe_{0.47})CO_3$ and $(Mg_{0.50}Mn_{0.50})CO_3$ at varied temperatures.

	T (K)	**a (Å)**	**c (Å)**	**V (Å^3)**	**M-O (Å)**	**C-O (Å)**	**O-M-O (Å)**	**V_{MO6} (Å^3)**
$Mg_{0.37}Mn_{0.32}Fe_{0.31}$-$CO_3$	100	4.6951(2)	15.3111(18)	292.3(4)	2.1429(7)	1.2860(14)	88.18(2)	13.11(7)
	200	4.6982(2)	15.3402(11)	293.24(3)	2.1455(6)	1.286(13)	88.135(19)	13.15(7)
	300	4.7015(2)	15.3673(9)	294.17(2)	2.1484(7)	1.2860(15)	88.11(2)	13.21(8)
	400	4.7041(2)	15.3993(8)	295.11(2)	2.1514(7)	1.2854(14)	88.068(19)	13.26(8)
	500	4.7067(2)	15.4217(9)	295.87(2)	2.1539(6)	1.2850(12)	88.050(17)	13.31(7)
$Fe_{0.51}Mg_{0.49}CO_3$	100	4.6566(2)	15.142(14)	284.35(3)	2.1178(6)	1.2863(12)	88.136(17)	12.65(7)
	200	4.6592(2)	15.1681(13)	285.16(3)	2.1209(5)	1.2850(10)	88.118(15)	12.71(6)
	300	4.6621(2)	15.1925(13)	285.97(3)	2.1237(5)	1.2841(10)	88.103(15)	12.76(6)
	400	4.6652(2)	15.2236(14)	286.94(3)	2.1267(6)	1.2840(12)	88.064(18)	12.81(7)
	500	4.6678(2)	15.2559(13)	287.87(3)	2.1299(6)	1.2829(11)	88.026(16)	12.87(7)
$Mn_{0.53}Fe_{0.47}CO_3$	100	4.7382(2)	15.4920(10)	301.21(3)	2.1703(9)	1.2863(17)	88.23(2)	13.62(9)
	200	4.7408(2)	15.5193(10)	302.07(3)	2.1731(8)	1.2855(16)	88.21(2)	13.67(8)
	300	4.7431(2)	15.5545(9)	303.05(3)	2.1766(8)	1.2840(17)	88.17(2)	13.73(8)
	400	4.7458(2)	15.5661(8)	303.62(2)	2.1789(8)	1.2830(16)	88.18(2)	13.78(8)
	500	4.7481(2)	15.5938(9)	304.45(3)	2.1818(8)	1.2820(16)	88.16(2)	13.83(8)
$Mg_{0.50}Mn_{0.50}CO_3$	100	4.6991(2)	15.2948(10)	292.49(3)	2.1439(5)	1.2858(10)	88.270(14)	13.13(6)
	200	4.7011(2)	15.3244(10)	293.30(3)	2.1464(5)	1.2855(10)	88.223(15)	13.17(6)
	300	4.7038(2)	15.3526(10)	294.18(3)	2.1489(5)	1.2855(11)	88.183(15)	13.22(6)
	400	4.7065(2)	15.3881(11)	295.20(3)	2.1525(6)	1.2843(12)	88.142(17)	13.28(7)
	500	4.7090(2)	15.4088(10)	295.91(3)	2.1548(5)	1.2837(11)	88.128(15)	13.33(6)